Available online at www.sciencedirect.com

SciVerse ScienceDirect

Ceramics International 38 (2012) 6495–6499

CERAMICS INTERNATIONAL

www.elsevier.com/locate/ceramint

The effects of nanoparticle addition on the sintering and properties of bimodal AlN

Valmikanathan P. Onbattuvelli[a], Ravi K. Enneti[b], Sundar V. Atre[a,*]

[a]Oregon State University, Corvallis, OR, USA
[b]Global Tungsten and Powders Corporation, Towanda, PA, USA

Received 28 March 2012; received in revised form 8 May 2012; accepted 9 May 2012
Available online 5 June 2012

Abstract

The effects of nanoparticle addition on the pressureless sintering of injection molded and debound aluminum nitride (AlN) samples were studied. Variations in the densification, microstructure, and properties owing to the increased powder content and reduced particle size are discussed. The results indicate the formation of liquid phase at 1500 °C in the bimodal micro (μ)–nano (n) AlN samples, a temperature that is at least 100 °C lower than typically reported values in the literature. Consequently, a densification $\geq$ 99% was achieved by pressureless sintering at a relatively lower temperature of 1650 °C with ~14% isometric shrinkage. Additionally, thermal and mechanical properties of the sintered bimodal AlN samples are presented and compared with sintering studies on conventional monomodal μ-AlN systems reported in the literature.

Keywords: Aluminum nitride; Nanoparticles; Shrinkage; Weight loss

1. Introduction

Aluminum nitride (AlN) has attracted considerable attention as a substrate material for electronic packaging because of its excellent properties, such as high thermal conductivity and coefficient of thermal expansion that are well matched to that of silicon [1–4]. These properties make AlN an excellent material to replace alumina (Al_2O_3) and beryllia (BeO) used for the manufacture of semiconductor devices [5,6]. AlN also has the potential to be used as heat sinks for high operating temperature applications, LED thermal management, laser diode heat spreaders, optoelectronic parts, cutting tools, ignition modules, and casting crucibles [5–8]. In order to translate the above mentioned thermal properties into demanding applications, it is necessary to net-shape AlN into fully dense microstructures.

Prior reports investigated AlN densification by exploring material and process parameters. AlN is a covalently-bonded material and requires sintering additives to enhance densification. Thus, prior reports on material parameters focused on the effect of varying the type and amount of sintering additives on the densification behavior of AlN. For example, Surnev et al. studied the effect of varying the amount of yttria (Y_2O_3) as the sintering aid over the final density [9]. Similarly, Molisani et al. compared the efficiency of Y_2O_3 and calcium oxide (CaO), as sintering aids for AlN densification [10]. Sintering temperature and hold time were the commonly studied process parameters in the past. For example, Zhou et al. [11] and Li et al. [12] reported the increase in the sintered density with the increase in the sintering temperature. On the other hand, Kume et al. noticed a decrease in the sintered density with higher hold time at the sintering temperature [13]. A brief literature review on AlN densification is presented by our research group elsewhere [14].

One research issue that is least explored till date is the effect of initial powder packing density on the final sintered density of AlN ceramics [15]. Our prior research work successfully demonstrated an increase in powder content with the addition of nanoparticles, forming bimodal μ–n powder mixtures [16,17]. For example, the powder content was found to increase from 54 to 71 vol% when

---

*Corresponding author. Tel.: +1 541 908 1483.
E-mail address: Sundar.Atre@oregonstate.edu (S.V. Atre).

0272-8842/$36.00 © 2012 Elsevier Ltd and Techna Group S.r.l. All rights reserved.
http://dx.doi.org/10.1016/j.ceramint.2012.05.028

AlN nanoparticles are added to the monomodal submicron (μ) sized AlN powders. The implication of nanoparticle additions has been discussed in the past in the context of powder–polymer mixture (feedstock) properties, mold filling behavior and polymer removal kinetics of the injection molded bimodal μ–n AlN and SiC samples [16,18]. In a similar manner, the effect of nanoparticle addition on the sintering behavior of AlN at different time–temperature combinations is discussed in the current paper. Y_2O_3 is the most commonly reported sintering additive for AlN and is thus used in the current study [1–4,9,10,15]. These sintering experiments reveal that bimodal μ–n AlN powder mixtures display liquid phase formation at relatively lower temperatures. The sintered density, shrinkage, thermal and mechanical properties of the resulting sintered bimodal μ–n samples are compared with that of the previously reported sintering studies on conventional monomodal μ–AlN samples.

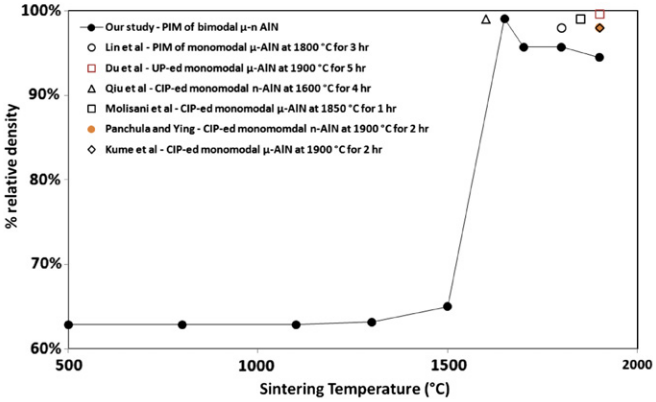

Fig. 1. Effect of sintering temperature on the pressureless densification of AlN.

2. Experimental section

The starting powder materials contain as-received, commercially available AlN (1.1 μm and 20 nm) with 5 wt% Y_2O_3 (50 nm) as the sintering additive. Powder injection molded bimodal μ–n AlN samples were solvent and thermally debound prior to sintering. The molding and debinding conditions used are detailed elsewhere [16,18]. Thermally debound bimodal AlN samples with an initial density of 2.15 g/cc (65% relative density) were pressureless sintered at different temperatures up to 1900 °C for 4 h under nitrogen atmosphere. The density for all the sintered samples was measured with a lab-built Archimedes apparatus. Microstructural analysis was conducted on the fracture surfaces of sintered AlN samples using a Quanta TM—FEG (FEI) dual beam scanning electron microscope (SEM) coupled with an energy dispersive X-ray spectrometer (EDS). SEM images of each sample were presented in two different magnifications for better comparison. The thermal diffusivity of the samples was measured with an LFA-457 (Netzsch) laser flash apparatus. TA Instruments-2920 unit was used to measure the specific heat (Cp) of the sintered samples. Vickers hardness and indentation toughness of the sintered AlN samples were measured via Leco microhardness tester.

3. Results and discussion

The progress in densification of bimodal μ–n AlN with increase in sintering temperature is shown in Fig. 1. From Fig. 1 it can be seen that the densification of the bimodal μ–n AlN is initiated at 1500 °C. The SEM micrographs of the samples at various sintering temperatures are shown in Figs. 2 and 3. The micrographs shown in Fig. 2 confirm liquid phase formation at1500 °C. The onset of liquid phase formation in the present study is comparatively lower by at least 100 °C than observations in prior reports using monomodal μ–AlN [1,3,9,15,21,22]. A shift in densification towards lower sintering temperatures can be attributed to the early formation of liquid phase. A density ≥ 99% was obtained for samples sintered at 1650 °C (Fig. 3a). In comparison, densification to 95% at 1600 °C has been previously reported by Panchula and Ying for a monomodal n-AlN system [23]. They proposed two likely mechanisms that could be responsible for the low-temperature densification of ultrafine AlN systems. Firstly, an Al–Y–O–N liquid could form and promote material transport via liquid-phase sintering. Secondly, solid-state grain boundary diffusion could increase due to the higher surface area of n-AlN, which in turn expedites Y_2O_3 doping at the grain boundaries. This hypothesis is supported by the AlN grain growth with increase in sintering temperature observed in the present study (Fig. 3b–d). The densification of AlN is presumed to occur by liquid phase sintering, accompanied by solution-reprecipitation between the AlN and the liquid phase [6]. AlN typically contains dissolved oxygen in its lattice. At lower temperatures, this dissolved oxygen is hypothesized to exist in the form of aluminum oxynitride, $Al_9N_7O_3$. These oxygen impurities diffuse through the grain boundary to react with Y_2O_3, forming yttrium aluminates with a smaller yttrium-to-aluminum atomic ratio Y/Al [6,19–21]. Zhou et al. [11] postulated that during AlN sintering, $Y_4Al_2O_9$ is first formed. At high temperatures, the major secondary phases were found to be $YAlO_3$ and $Y_3Al_5O_{12}$ (yttrium aluminum garnet—YAG). In particular, YAG formation results in reduction in oxygen vacancies, which in turn enhances the growth of AlN grains.

A decrease in weight loss of 6.92 ± 1.67 wt% corresponding to decrease in density was observed at sintering temperatures above 1650 °C. Such weight loss has previously been attributed to the breakdown of $YAlO_3$ yielding volatile monoxides of Al and Y along with O_2. The $YAlO_3$ itself is formed due to reaction between the excess Y_2O_3 present in the mixture with the YAG at elevated temperatures [10]. This material loss would open up new pores at sintering temperatures leading to reduction in density. Similar results on AlN densification have been qualitatively analyzed in the past by Molisani et al. [10],

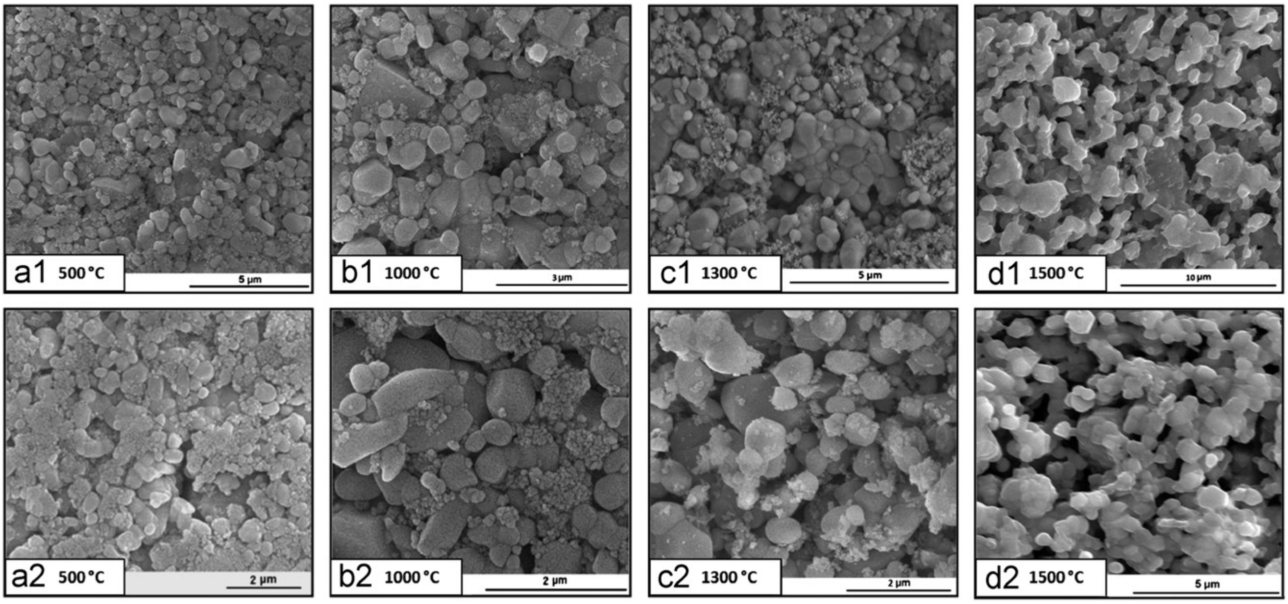

Fig. 2. SEM images revealing the transition of bimodal μ–n AlN samples from thermally debound stage to the onset of liquid phase formation.

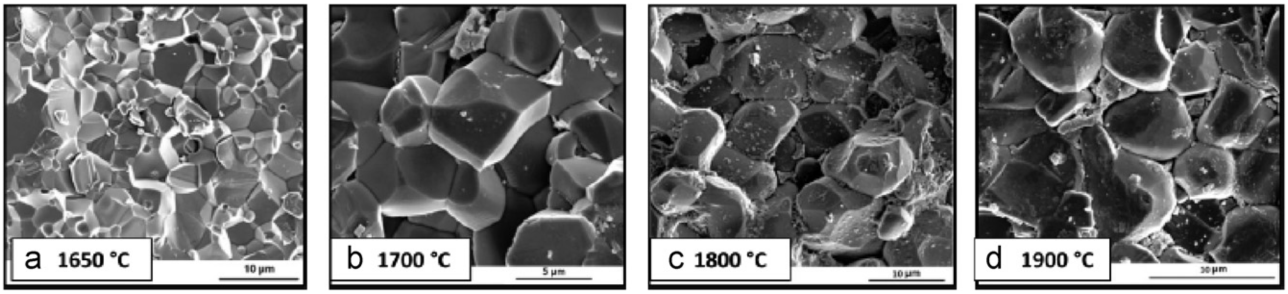

Fig. 3. SEM images revealing the grain growth in the bimodal μ–n AlN samples with the increase in the sintering temperatures.

Panchula and Ying [23] and Olhero et al. [24] arguing the necessity to optimize the Y_2O_3 content prior to AlN sintering. Future experiments including TGA-assisted-mass spectroscopy and XRD analysis are required to explain the effect of nanoparticle addition on the weight loss in the bimodal μ–n AlN samples.

The variation of shrinkage of the samples with sintering temperature is shown in Fig. 4. The plot is also extended to compare the shrinkage reported in the literature for monomodal μ-AlN densification [1,22,24,25]. An isometric shrinkage of up to 14% was noticed in the samples from the present study corresponding to 99% densification. The shrinkage observed in the bimodal μ–n AlN samples is significantly lower than for the monomodal μ-AlN samples reported in literature. The high powder packing density and ability for densification at lower temperatures due to nanoparticle addition are the most likely reasons for the observed lower shrinkage. This result confirms the value of bimodal μ–n powder mixtures in obtaining lower shrinkage following complete densification. It is anticipated that the reduced sintering shrinkage can, in principle, lead to better dimensional control in sintered parts.

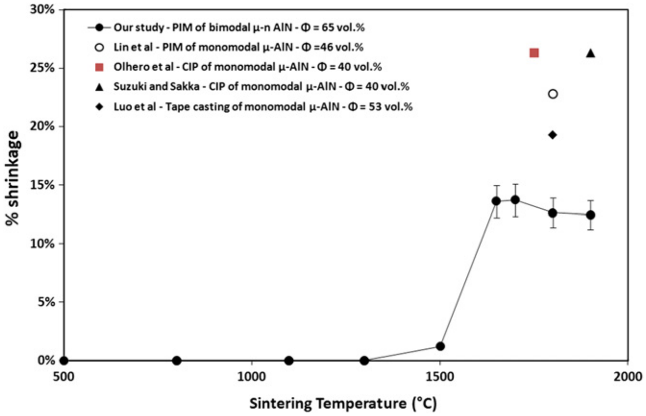

Fig. 4. Effect of sintering temperature on shrinkage during AlN densification.

Fig. 5 plots the thermal diffusivity values of samples at different sintering temperature. The thermal diffusivity of the bimodal μ–n AlN is expected to increase with temperature due to the grain growth. In contrast, fluctuations

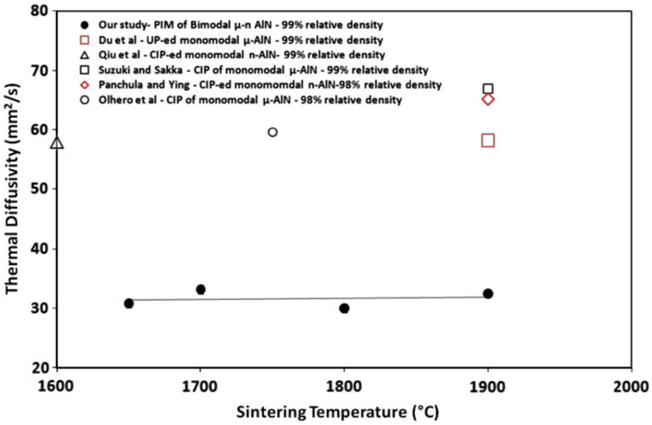

Fig. 5. Thermal diffusivity of AlN samples as a function of sintering temperature.

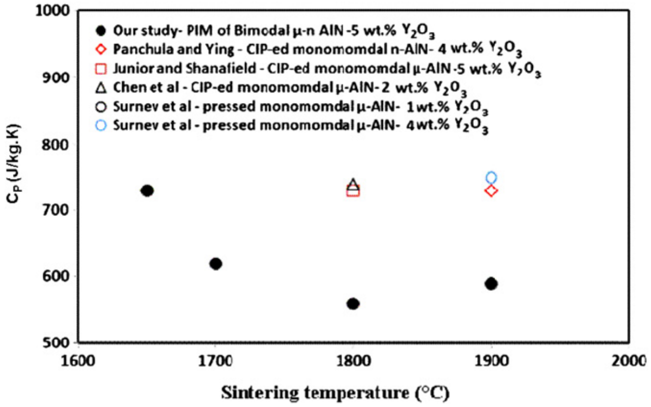

Fig. 6. *C*p of AlN samples as a function of sintering temperature.

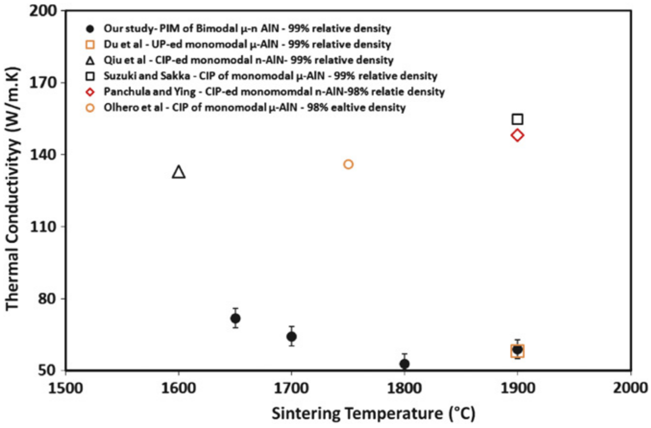

Fig. 7. Thermal conductivity of AlN samples as a function of sintering temperature.

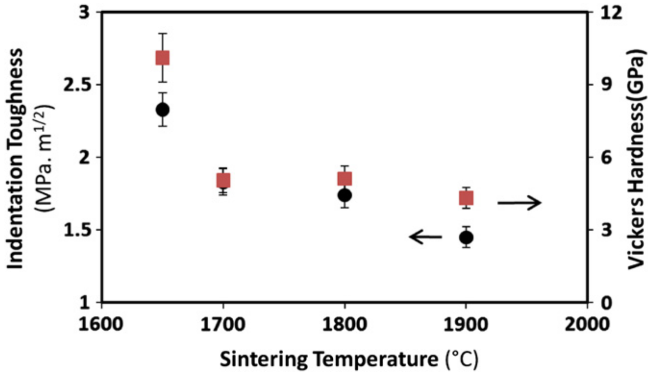

Fig. 8. Mechanical properties of bimodal μ–n AlN samples as a function of sintering temperature.

were noticed which could be explained as the combined outcome of simultaneous grain boundary loss and weight loss. A maximum thermal diffusivity of 33 mm^2/s is noticed for the bimodal μ–n AlN samples sintered at 1700 °C and 1900 °C. Suzuki and Sakka [22] and Olhero et al. [24] previously reported a similar trend for monomodal μ-AlN samples. In addition to the weight loss explained earlier, the use of excessive amount of nanoscale sintering additives could be detrimental to the sintered properties possibly due to higher content of inter-granular glassy phase. The variation of heat capacity (C_p) of the samples with sintering temperatures is shown in Fig. 6. A higher C_p value was observed for bimodal μ–n samples sintered at 1650 °C. The C_p of bimodal μ–n samples at 1650 °C was similar to the values reported in literature for monomodal μ-AlN at 1800 °C and 1900 °C. However, the C_p values of bimodal μ–n samples decreased with further increase in sintering temperature above 1650 °C, possibly correlating with the reduced sintered density and increased grain growth.

The thermal conductivity (K) value of samples in the present study at different sintering temperatures is shown in Fig. 7. The observed thermal conductivity for the bimodal μ–n samples was considerably lower than the monomodal μ-AlN reported in literature. The thermal conductivity is a product of thermal diffusivity, sintered density and C_p. Thus, factors such as sintered density, weight loss, grain growth and amount of inter-granular glassy phase can affect the thermal conductivity of the given samples. In addition to these factors, the oxygen content also has significant effect on the thermal conductivity [26,27]. Despite the fact that bimodal μ–n AlN samples revealed ≥ 99% densification, the higher amount of liquid phase additives, smaller grain size and higher weight loss could account for the lower thermal conductivity values. A detailed analysis with variations in the fabrication techniques and amount and composition of sintering aids is required to explore the possibility to increase the thermal conductivity values of bimodal μ–n AlN.

The variation in Vickers hardness and indentation toughness of bimodal μ–n AlN samples is shown in Fig. 8. A maximum Vickers hardness of 10.2 GPa and indentation toughness of 2.3 MPa .m$^{1/2}$ were observed for the bimodal μ–n AlN samples sintered at 1650 °C. Similar values of hardness equivalent to 11.5 GPa and toughness of 3 MPa .m$^{1/2}$ were reported in the past for different compositions of monomodal μ-AlN [28–30]. Additionally, as shown in Fig. 8, both the Vickers hardness and indentation toughness reduced with increase in temperatures, possibly due to lower sintered density.

4. Conclusions

Bimodal μ–n AlN samples exhibited liquid phase formation at lower temperatures compared to that of conventional monomodal μ-AlN samples. Correspondingly, a shift in densification to a relatively lower sintering temperature as well as reduced isometric shrinkage was also observed. The combined effects of increased powder content and reduced average particle size by nanoparticle addition are proposed as the reason for such behavior. Lower thermal diffusivity and thermal conductivity values were observed for the bimodal μ–n AlN compared to monomodal μ-AlN systems reported in the literature. It is suggested that these differences are the possible outcome of the weight loss during sintering despite AlN densification and grain growth. Mechanical properties of the bimodal μ–n AlN systems were comparable to those observed for monomodal μ-AlN. Further, a reduction was noticed in the mechanical properties with the increase in the sintering temperatures that correlated with the density and microstructural evolution.

References

[1] K.H. Lin, Y.C. Lin, S.T. Lin, Effects of reduction atmosphere and nano carbon powder addition on the deoxidization of injection molded aluminum nitride parts, Journal of Materials Processing Technology 201 (2008) 701–705.

[2] A.F. Junior, D. Shanafield, The use of yttrium (III) isopropoxide to improve thermal conductivity of polycrystalline aluminum nitride (AlN) ceramics, Journal of Materials Science: Materials in Electronics 16 (2005) 139–144.

[3] M. Medraj, Y. Baik, W.T. Thompson, R.A.L. Drew, Understanding AlN sintering through computational thermodynamics combined with experimental investigation, Journal of Materials Processing Technology 161 (2005) 415–422.

[4] X. Du, M. Qin, F. Akhtar, P. Fengg, X. Qu, Effects of heat treatment on the properties of powder injection molded AlN ceramics, Rare Metals 27 (2008) 70–73.

[5] Y. Baik, R.A.L. Drew, Aluminum nitride: processing and applications, Key Engineering Materials 122–124 (1996) 553–570.

[6] A.V. Virkar, T.B. Jackson, K.L. More, R.A. Cutler, High-thermal-conductivity aluminum nitride ceramics: the effect of thermodynamic, kinetic, and microstructural factors, Journal of the American Ceramic Society 80 (1997) 1421–1435.

[7] D. Palit, A.M. Meier, Reaction kinetics and mechanical properties in the reactive brazing of copper to aluminum nitride, Journal of Materials Science 41 (2006) 7197–7209.

[8] I.-L. Tangen, Y. Yu, T. Grande, R. Hoier, M.-A. Einarsrud, Phase relations and microstructural development of aluminum nitride–aluminum nitride polytypoid composites in the aluminum nitride–alumina–yttria System, Journal of the American Ceramic Society 87 (2004) 1734–1740.

[9] S. Surnev, D. Lepkova, A. Yoleva, Influence of the sintering additives on the phase composition and the thermal conductivity of aluminum nitride ceramics, Materials Science and Engineering B: Advanced Functional Solid-State Materials 10 (1991) 35–40.

[10] A.L. Molisani, H.N. Yoshimura, H. Goldenstein, K. Watari, Effects of $CaCO_3$ content on the densification of aluminum nitride, Journal of the European Ceramic Society 26 (2006) 3431–3440.

[11] H. Zhou, Y. Liu, W. Miao, Y. Wu, Effects of binary additives B_2O_3–Y_2O_3 on the microstructure and thermal conductivity of aluminum nitride ceramics, Journal of Materials Science 34 (1999) 6165–6168.

[12] X.L. Li, H.A. Ma, Y.J. Zheng, Y. Liu, G.H. Zuo, W.Q. Liu, J.G. Li, X. Jia, AlN ceramics prepared by high-pressure sintering with La_2O_3 as a sintering aid, Journal of Alloys and Compounds 463 (2008) 412–416.

[13] S. Kume, M. Yasuoka, N. Omura, K. Watari, Effects of annealing on dielectric loss and microstructure of aluminum nitride ceramics, Journal of the American Ceramic Society 88 (11) (2005) 3229–3231.

[14] V.P. Onbattuvelli, S.V. Atre, Review of net shape fabrication of thermally conducting ceramics, Materials and Manufacturing Processes 26 (6) (2011) 832–845.

[15] J.Y. Qiu, Y. Hotta, K. Watari, Enhancement of densification and thermal conductivity in AlN ceramics by addition of nano-Sized particles, Journal of the American Ceramic Society 89 (1) (2006) 377–380.

[16] V. Onbattuvelli, S. Vallury, S. Laddha, S. Atre, Properties of SiC and AlN feedstocks for the powder injection moulding of thermal management devices, PIM International 4 (3) (2010) 64–70.

[17] V. Onbattuvelli, G. Purdy, G. Kim, S. Laddha, S. Atre, Powder injection molding of bimodal μ–n silicon carbide and aluminum nitride ceramics, Advances in Powder Metallurgy and Particulate Materials 1 (2010) 64–72.

[18] V. Onbattuvelli, G. Purdy, G. Kim, S.J. Park, S. Atre, Journal of the American Ceramic Society 2011 (submitted).

[19] K. Watari, H.J. Hwang, M. Toriyama, S. Kanzaki, Effective sintering aids for low-temperature sintering of AlN ceramics, Journal of Materials Research 14 (1999) 1409–1417.

[20] K. Watari, H. Nakano, T. Tsugoshi, T. Nagaoka, K. Urabe, S. Cao, K. Mori, K. Ishizaki, Microstructure and thermal conductivity of AlN ceramic with eliminated grain boundary phase, Key Engineering Materials 247 (2003) 361–364.

[21] Masaki Shoichi Kume, Sang-Kee Yasuoka, Akinori Lee, Hirotaka Kan, Koji Ogawa, Watari, dielectric and thermal properties of AlN ceramics, Journal of the European Ceramic Society 27 (2007) 2967–2971.

[22] T.S. Suzuki, Y. Sakka, Preparation of oriented bulk 5 wt% Y_2O_3–AlN ceramics by slip casting in a high magnetic field and sintering, Scripta Materialia 52 (2005) 583–586.

[23] M.L. Panchula, J.Y. Ying, Nanocrystalline aluminum nitride: II, sintering and properties, Journal of the American Ceramic Society 86 (2003) 1121–1127.

[24] S.M. Olhero, P. Miranzo, J.M.F. Ferreira, Influence of the de-waxing atmosphere on the properties of AlN ceramic processed from aqueous media, Journal of the European Ceramic Society 26 (2006) 2475–2483.

[25] X. Luo, J. Li, B. Zhang, W. Li, H. Zhuang, High thermal conductivity aluminum nitride substrates prepared by aqueous tape casting, Journal of the American Ceramic Society 89 (3) (2006) 836–841.

[26] K. Watari, K. Ishizaki, T. Fujikawa, Thermal conduction mechanism of aluminum nitride ceramics, Journal of Materials Science 27 (1992) 2627–2630.

[27] K. Watari, H. Nakano, K. Urabe, K. Ishizaki, S. Cao, K. Mori, Thermal conductivity of AlN ceramic with a very low amount of grain boundary phase at 4 to 1000 K, Journal of Materials Research 17 (11) (2002) 2940–2944.

[28] Ferro-Ceramic Grinding Inc., MA, USA, Ceramic Components Directory, 2008, pp.13–14.

[29] J.W. McCauley, Weapons and Materials Research Directorate, 2002, ARL-TR-2740, p.8.

[30] F.M. Xu, Z.J. Zhang, X.L. Shia, Y. Tana, J.M. Yang, Effects of adding yttrium nitrate on the mechanical properties of hot-pressed AlN ceramics, Journal of Alloys and Compounds 509 (2011) 8688–8691.